

# CMIP5 ANALYSIS AND MODEL BENCHMARKING: Quantification and Reduction of Uncertainties Associated with Carbon Cycle–Climate System Feedbacks

Forrest M. Hoffman

Climate Change Science Institute (CCSI),  
Oak Ridge National Laboratory, Oak Ridge, Tennessee, USA

**PLUME-MIP Workshop**  
**East China Normal University, Shanghai, China**  
**September 26, 2015**

CLIMATE CHANGE  
SCIENCE INSTITUTE  
OAK RIDGE NATIONAL LABORATORY



# Research Questions

## Question 1

How well do Earth System Models (ESMs) simulate the observed distribution of anthropogenic carbon in atmosphere, ocean, and land reservoirs?

# Research Questions

## Question 1

How well do Earth System Models (ESMs) simulate the observed distribution of anthropogenic carbon in atmosphere, ocean, and land reservoirs?

## Question 2

Can contemporary atmospheric CO<sub>2</sub> observations be used to constrain future CO<sub>2</sub> projections?

# Research Questions

## Question 1

How well do Earth System Models (ESMs) simulate the observed distribution of anthropogenic carbon in atmosphere, ocean, and land reservoirs?

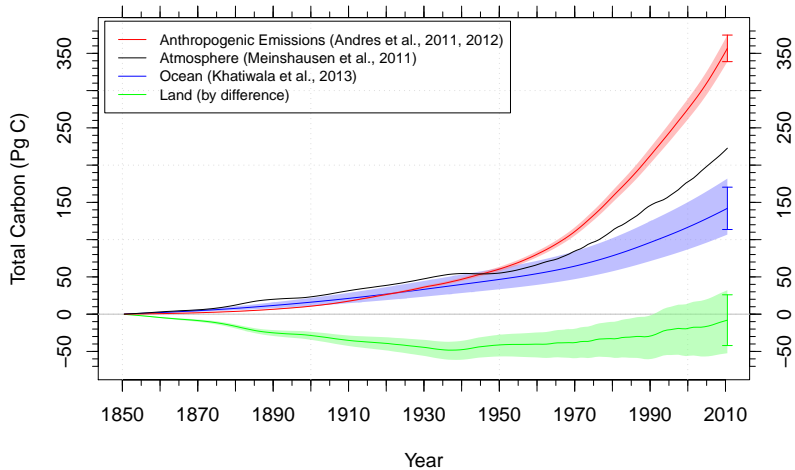
## Question 2

Can contemporary atmospheric CO<sub>2</sub> observations be used to constrain future CO<sub>2</sub> projections?

## Community Model Benchmarking

Systematic assessment of model fidelity, employing best-available observational data, can identify model weaknesses and inspire new measurements.

# Observed Carbon Accumulation Since 1850



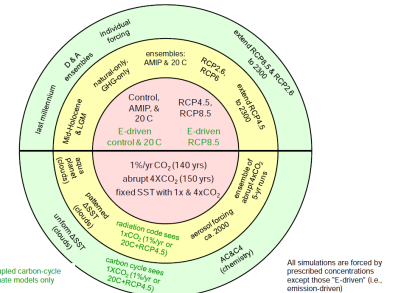
Observational estimates of anthropogenic carbon emissions (excluding land use change) and accumulation in atmosphere, ocean, and land reservoirs for 1850–2010. Atmosphere carbon is a fusion of Law Dome ice core CO<sub>2</sub> observations, the Keeling Mauna Loa record, and more recently the NOAA GMD global surface average, integrated for the purpose of forcing IPCC models. Total land flux is computed by mass balance as follows:

$$\Delta C_L = \sum_i F_i - \Delta C_A - \Delta C_O.$$

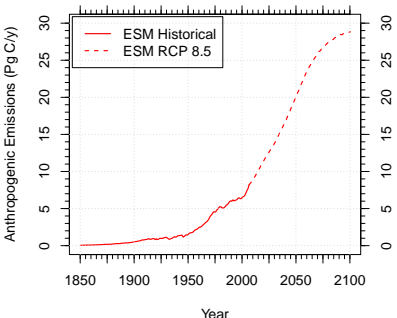
# CMIP5 Long-Term Experiments

15 fully-prognostic ESMs that performed CMIP5 emissions-forced simulations

Model	Modeling Center
BCC-CSM1.1	Beijing Climate Center, China Meteorological Administration, CHINA
BCC-CSM1.1(m)	Beijing Climate Center, China Meteorological Administration, CHINA
BNU-ESM	Beijing Normal University, CHINA
CanESM2	Canadian Centre for Climate Modelling and Analysis, CANADA
CESM1-BGC	Community Earth System Model Contributors, NSF-DOE-NCAR, USA
FGOALS-s2.0	LASG, Institute of Atmospheric Physics, CAS, CHINA
GFDL-ESM2g	NOAA Geophysical Fluid Dynamics Laboratory, USA
GFDL-ESM2m	NOAA Geophysical Fluid Dynamics Laboratory, USA
HadGEM2-ES	Met Office Hadley Centre, UNITED KINGDOM
INM-CM4	Institute for Numerical Mathematics, RUSSIA
IPSL-CM5A-LR	Institut Pierre-Simon Laplace, FRANCE
MIROC-ESM	Japan Agency for Marine-Earth Science and Technology, Atmosphere and Ocean Research Institute (University of Tokyo), and National Institute for Environmental Studies, JAPAN
MPI-ESM-LR	Max Planck Institute for Meteorology, GERMANY
MRI-ESM1	Meteorological Research Institute, JAPAN
NorESM1-ME	Norwegian Climate Centre, NORWAY

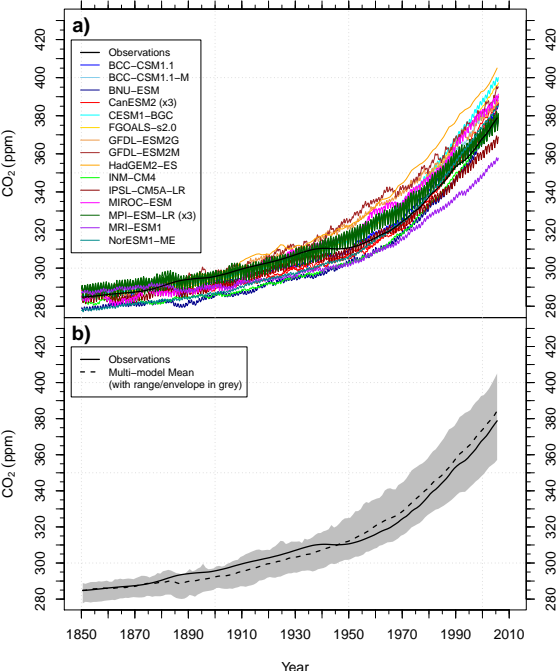


## Emissions for Historical + RCP 8.5 Simulations



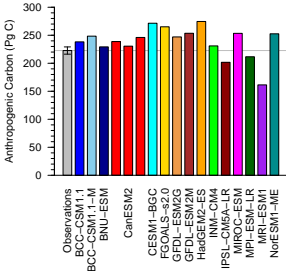
## ESM Historical Atmospheric CO<sub>2</sub> Mole Fraction

(a) Most ESMs exhibited a high bias in predicted atmospheric CO<sub>2</sub> mole fraction, which ranged from 357–405 ppm at the end of the historical period (1850–2005).



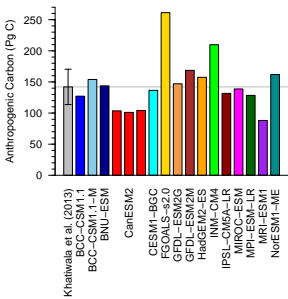
# Model inventory comparison with Khatiwala et al. (2013)

Atmosphere (1850–2010)



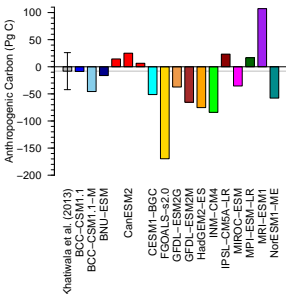
Once normalized by their atmospheric carbon inventories, most ESMs exhibited a low bias in anthropogenic ocean carbon accumulation through 2010.

Ocean (1850–2010)

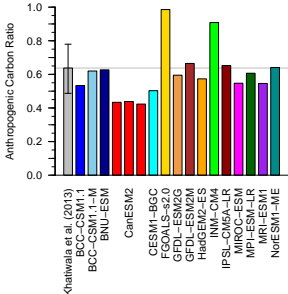


The same pattern holds for the Sabine et al. (2004) inventory derived using the  $\Delta C^*$  separation technique.

Land (1850–2010)

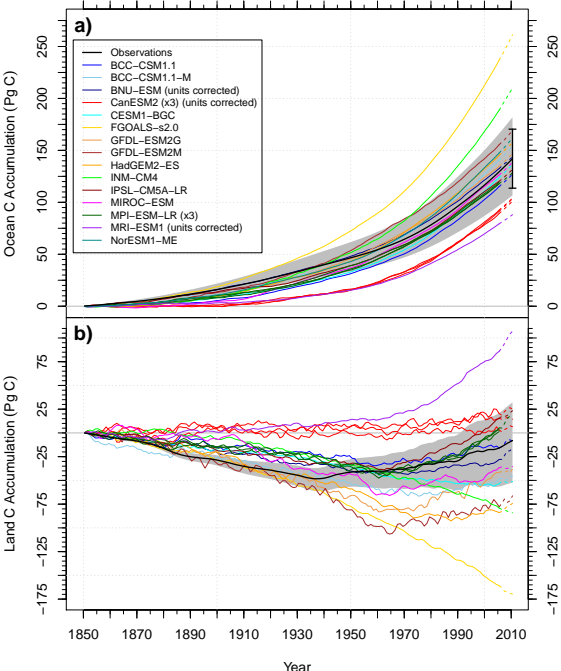


Ocean/Atmosphere (1850–2010)



## ESM Historical Ocean and Land Carbon Accumulation

(a) Ocean inventory estimates had a fairly persistent ordering during the second half of the 20<sup>th</sup> century.

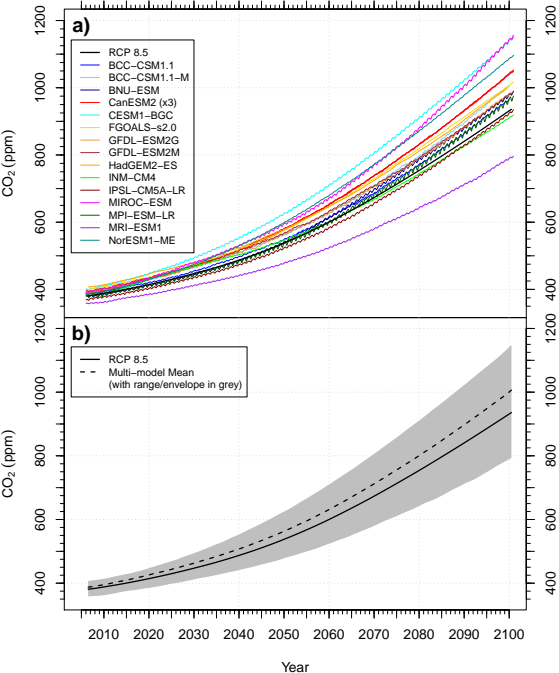


## Question 1

How well do Earth System Models (ESMs) simulate the observed distribution of anthropogenic carbon in atmosphere, ocean, and land reservoirs?

- ▶ Most ESMs exhibited a high bias in predicted atmospheric CO<sub>2</sub> mole fraction, ranging from 357–405 ppm in 2005.
- ▶ The multi-model mean atmospheric CO<sub>2</sub> mole fraction was biased high from 1946 onward, ending 5.6 ppm above observations in 2005.
- ▶ Once normalized by atmospheric carbon accumulation, most ESMs exhibited a low bias in ocean accumulation in 2010.
- ▶ ESMs predicted a wide range of land carbon accumulation in response to increasing CO<sub>2</sub> and land use change, ranging from –170–107 Pg C in 2010.

## ESM RCP 8.5 Atmospheric CO<sub>2</sub> Mole Fraction



### Question 2

Can contemporary atmospheric CO<sub>2</sub> observations be used to constrain future CO<sub>2</sub> projections?

## Reducing Uncertainties Using Observations

To reduce feedback uncertainties using contemporary observations,

1. there must be a relationship between contemporary variability and future trends on longer time scales within the model, and

# Reducing Uncertainties Using Observations

To reduce feedback uncertainties using contemporary observations,

1. there must be a relationship between contemporary variability and future trends on longer time scales within the model, and
2. it must be possible to constrain contemporary variability in the model using observations.

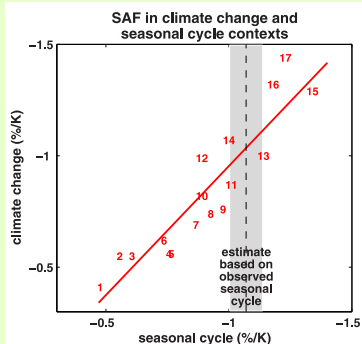
# Reducing Uncertainties Using Observations

To reduce feedback uncertainties using contemporary observations,

1. there must be a relationship between contemporary variability and future trends on longer time scales within the model, and
2. it must be possible to constrain contemporary variability in the model using observations.

## Example #1

Hall and Qu (2006) evaluated the strength of the springtime snow albedo feedback (SAF;  $\Delta\alpha_s/\Delta T_s$ ) from 17 models used for the IPCC AR4 and compared them with the observed springtime SAF from ISCCP and ERA-40 reanalysis.



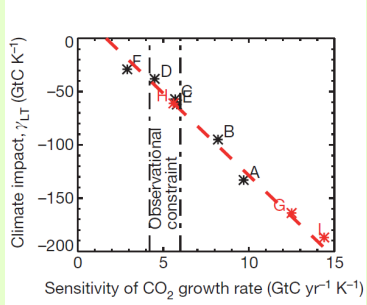
# Reducing Uncertainties Using Observations

To reduce feedback uncertainties using contemporary observations,

1. there must be a relationship between contemporary variability and future trends on longer time scales within the model, and
2. it must be possible to constrain contemporary variability in the model using observations.

## Example #2

Cox et al. (2013) used the observed relationship between the CO<sub>2</sub> growth rate and tropical temperature as a constraint to reduce uncertainty in the land carbon storage sensitivity to climate change ( $\gamma_L$ ) in the tropics using C<sup>4</sup>MIP models.

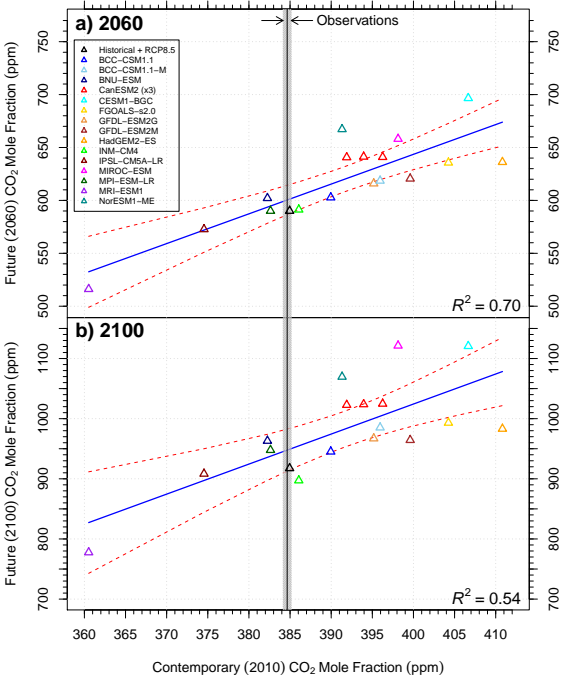


## Future vs. Contemporary Atmospheric CO<sub>2</sub> Mole Fraction

I developed a new emergent constraint from carbon inventories.

A relationship exists between contemporary and future atmospheric CO<sub>2</sub> levels over decadal time scales because carbon model biases persist over decadal time scales.

Observed contemporary atmospheric CO<sub>2</sub> mole fraction is represented by the vertical line at  $384.6 \pm 0.5$  ppm.

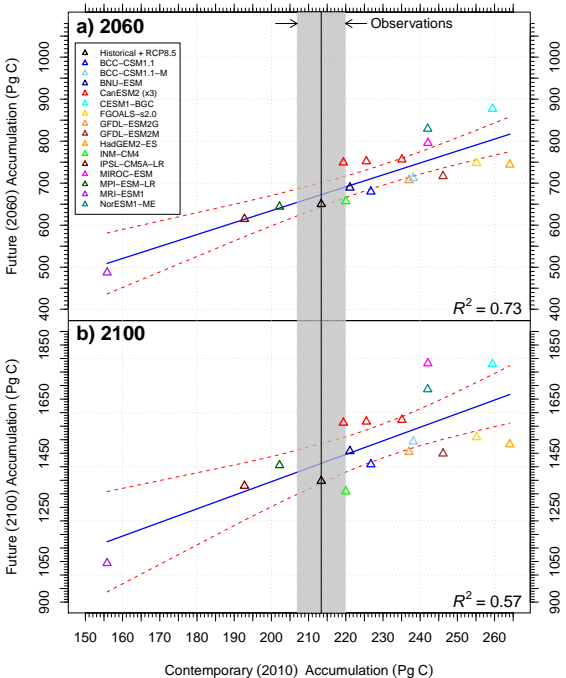


Removing pre-industrial CO<sub>2</sub> mole fraction biases from models, we found the relationship held, confirming the robustness of our result.

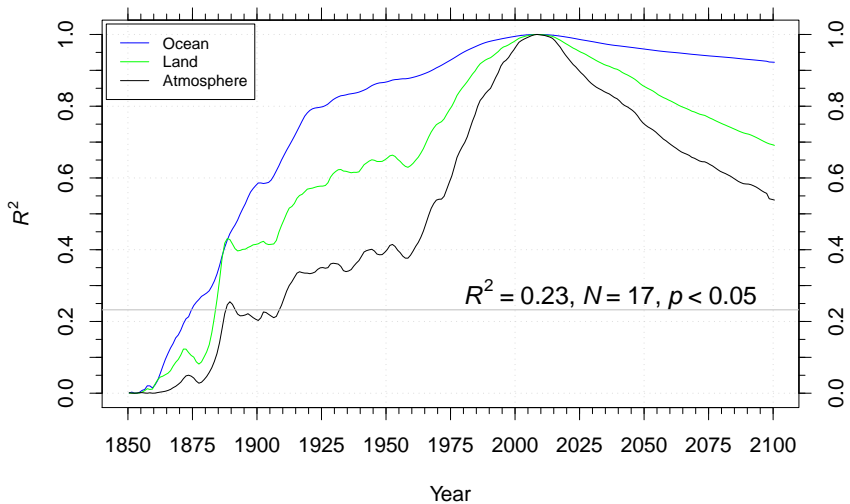
Observed contemporary anthropogenic atmospheric carbon inventory is represented by the vertical line at  $213.4 \pm 6.5$  Pg C, which incorporates 1850 CO<sub>2</sub> mole fraction uncertainties.

Adding uncertainties from fossil fuel emissions increased the uncertainty to  $\pm 12.7$  Pg C.

## Future vs. Contemporary Atmospheric Accumulation

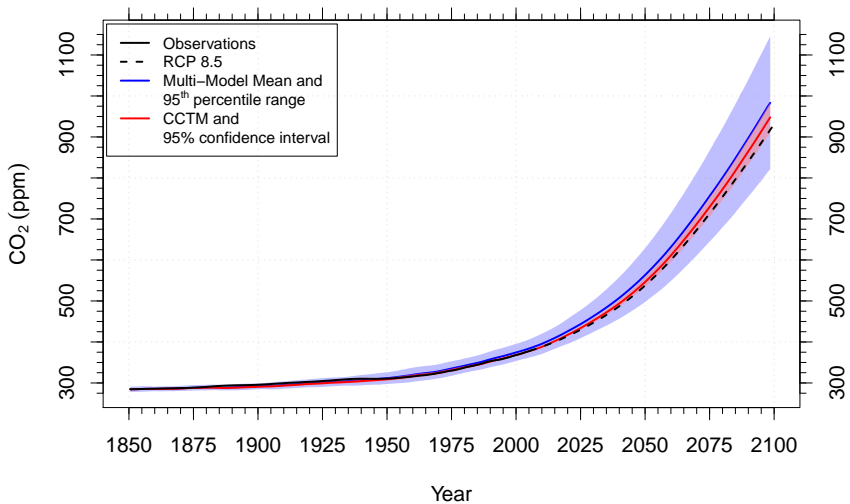


## $R^2$ of Multi-model Bias Structure



The coefficients of determination ( $R^2$ ) for the multi-model bias structure relative to the set of CMIP5 model atmospheric CO<sub>2</sub> mole fractions (black), and oceanic (blue) and land (green) anthropogenic carbon inventories in 2010. Atmospheric CO<sub>2</sub> mole fractions are statistically significant for 1910–2100. Bias persistence was highest for the ocean, followed by land, and then by the atmosphere.

# Contemporary CO<sub>2</sub> Tuned Model (CCTM)



I used this regression to create a contemporary CO<sub>2</sub> tuned model (CCTM) estimate of the atmospheric CO<sub>2</sub> trajectory for the 21<sup>st</sup> century.

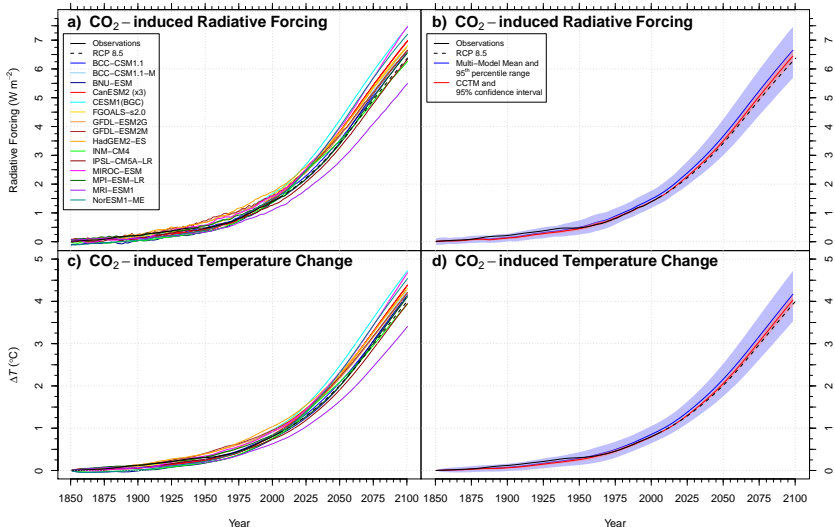
**Best estimate developed using Mauna Loa CO<sub>2</sub> data:**

**At 2060:**  $600 \pm 14$  ppm, 21 ppm below the multi-model mean

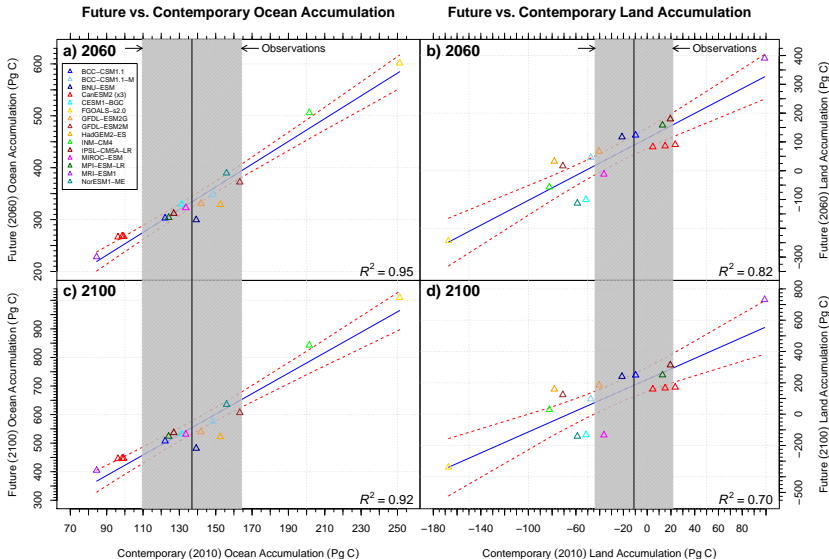
**At 2100:**  $947 \pm 35$  ppm, 32 ppm below the multi-model mean

### Projections for Individual CMIP5 Models

### CCTM Relative to the Multi – Model Mean



I calculated the CO<sub>2</sub> radiative forcing and used an impulse response function (tuned to the mean transient climate response of CMIP5 models) to equitably compute the resulting CO<sub>2</sub>-induced temperature change ( $\Delta T_{CO_2}$ ) for models and the CCTM. The CO<sub>2</sub> biases for individual models contributed to  $\Delta T_{CO_2}$  biases of  $-0.7^{\circ}C$  to  $+0.6^{\circ}C$  by 2100, relative to the CCTM estimate.



I also developed a multi-model constraint on the evolution of ocean and land anthropogenic inventories. Since observational uncertainties are higher for ocean and land, uncertainties in future estimates cannot be reduced as much as for atmospheric CO<sub>2</sub>.

## Question 2

Can we use contemporary CO<sub>2</sub> observations to constrain future CO<sub>2</sub> projections?

- ▶ Yes.
- ▶ I developed a new emergent constraint from anthropogenic carbon inventories in atmosphere, ocean, and land reservoirs.
- ▶ Land and ocean processes contributing to contemporary carbon cycle biases persist over decadal timescales.
- ▶ I used the relationship between contemporary and future atmospheric CO<sub>2</sub> levels to create a contemporary CO<sub>2</sub> tuned model (CCTM) estimate for the 21<sup>st</sup> century.
  - ▶ At 2060:  $600 \pm 14$  ppm, 21 ppm below the multi-model mean.
  - ▶ At 2100:  $947 \pm 35$  ppm, 32 ppm below the multi-model mean.
- ▶ Uncertainties in future climate predictions may be reduced by improving models to match the long-term time series of CO<sub>2</sub> from Mauna Loa and other monitoring stations.

# Implications of CO<sub>2</sub> Biases in ESMs

- Most of the model-to-model variability of CO<sub>2</sub> in the 21<sup>st</sup> century was traced to biases that existed at the end of the observational record.
- Future fossil fuel emissions targets designed to stabilize CO<sub>2</sub> levels would be too low if estimated from the multi-model mean of ESMs.
- Models could be improved through extensive comparison with observations and community model benchmarking.

@AGU PUBLICATIONS



Journal of Geophysical Research: Biogeosciences

RESEARCH ARTICLE

10.1002/2013JG002381

For PEER REVIEWED

Manuscript received 15 January 2013

Revised 15 March 2013

Accepted 20 March 2013

Published online 11 April 2013

Editorial

Editor-in-Chief

Volume 119, Number 2

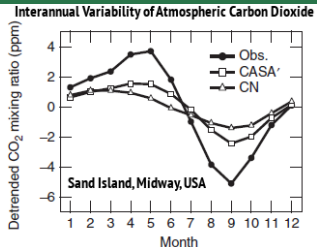
DOI: 10.1002/jgrb

ISSN: 2369-6493

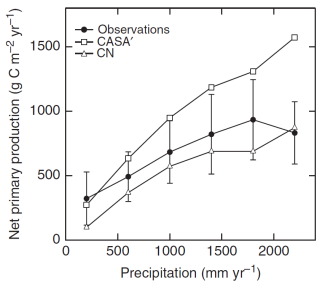
ISSN: 236

# What is a Benchmark?

- ▶ A **Benchmark** is a quantitative test of model function achieved through comparison of model results with observational data.
- ▶ Acceptable performance on benchmarks **is a necessary but not sufficient condition** for a fully functioning model.
- ▶ **Functional benchmarks** offer tests of model responses to forcings and yield insights into ecosystem processes.
- ▶ Effective benchmarks must draw upon a broad set of independent observations to evaluate model performance on **multiple temporal and spatial scales**.



Models often fail to capture the amplitude of the seasonal cycle of atmospheric CO<sub>2</sub>.



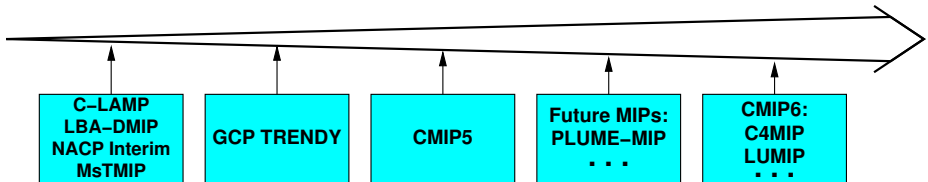
Models may reproduce correct responses over only a limited range of forcing variables.

(Randerson et al., 2009)

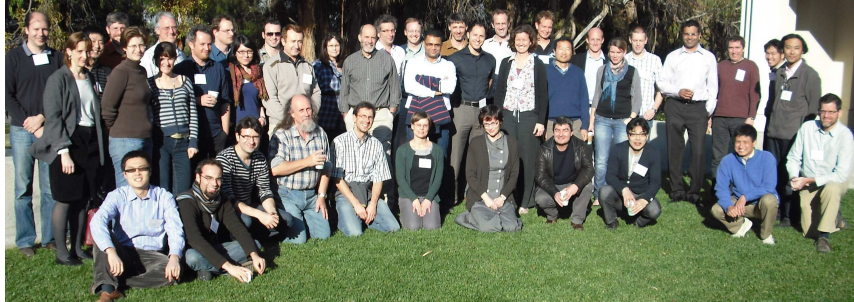
# Why Benchmark?

- ▶ to demonstrate to the science community and public that the representation of coupled climate and biogeochemical cycles in Earth system models (ESMs) is improving;
- ▶ to quantitatively diagnose impacts of model development in related fields on carbon cycle processes;
- ▶ to guide synthesis efforts, such as the Intergovernmental Panel on Climate Change (IPCC), in the review of mechanisms of global change in models that are broadly consistent with available contemporary observations;
- ▶ to increase scrutiny of key datasets used for model evaluation;
- ▶ to identify gaps in existing observations needed for model validation;
- ▶ to accelerate incorporation of new measurements for rapid and widespread use in model assessment;
- ▶ to provide a quantitative, application-specific set of minimum criteria for participation in model intercomparison projects (MIPs).

# An Open Source Benchmarking Software System



- ▶ Human capital costs of making rigorous model-data comparisons is considerable and constrains the scope of individual MIPs.
- ▶ Many MIPs spend resources “reinventing the wheel” in terms of variable naming conventions, model simulation protocols, and analysis software.
- ▶ **Need for ILAMB:** Each new MIP has access to the model-data comparison modules from past MIPs through ILAMB (e.g., MIPs use one common modular software system). Standardized international naming conventions also increase MIP efficiency.



## International Land Model Benchmarking (ILAMB) Meeting The Beckman Center, Irvine, CA, USA January 24-26, 2011



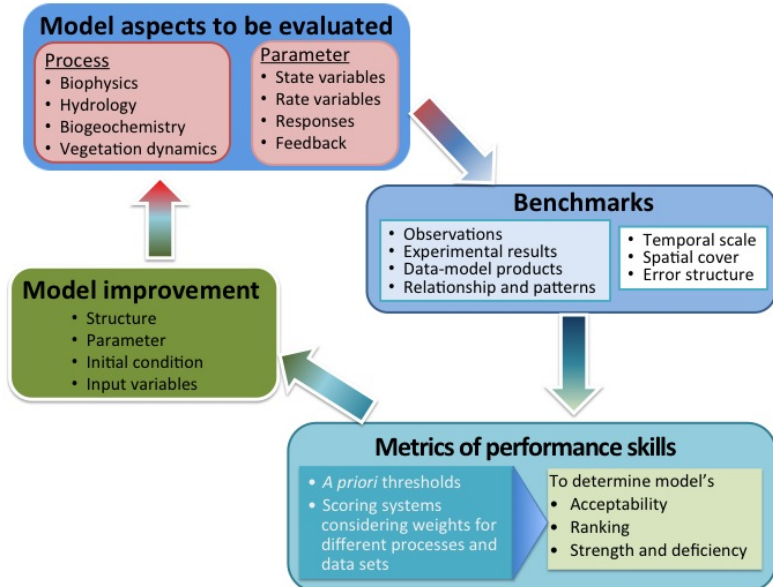
GLOBAL  
IGBP  
CHANGE  
International  
Globosphere-Biosphere  
Programme



DEPARTMENT OF EARTH SYSTEM SCIENCE  
SCHOOL OF PHYSICAL SCIENCES  
UNIVERSITY OF CALIFORNIA • IRVINE

- We co-organized inaugural meeting and ~45 researchers participated from the United States, Canada, the United Kingdom, the Netherlands, France, Germany, Switzerland, China, Japan, and Australia.
- **ILAMB Goals:** Develop internationally accepted benchmarks for model performance, advocate for design of open-source software system, and strengthen linkages between experimental, monitoring, remote sensing, and climate modeling communities. *Initial focus on CMIP5 models.*
- Provides methodology for model–data comparison and baseline standard for performance of land model process representations (Luo et al., 2012).

# General Benchmarking Procedure



# Example Benchmark Score Sheet from C-LAMP

Models →

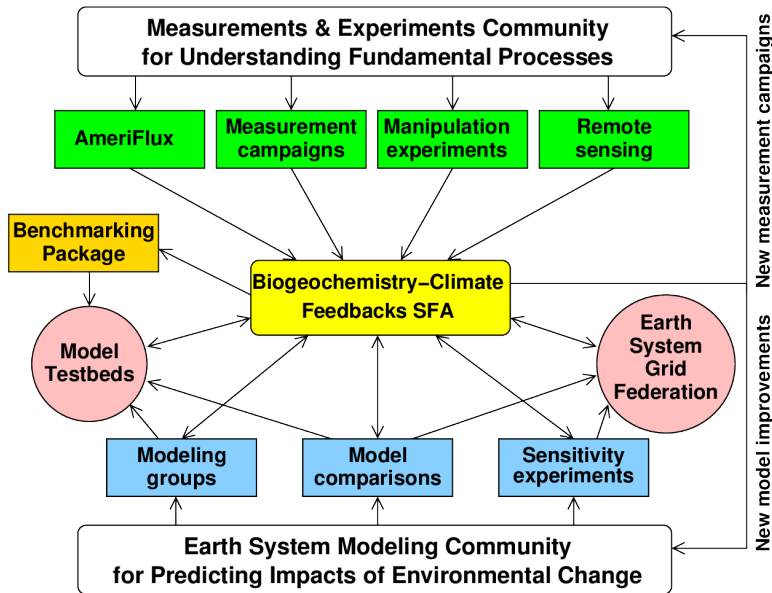
BGC Datasets ↓

Metric	Metric components	Uncertainty of obs.	Scaling mismatch	Total score	Sub-score	CASA'	CN
LAI	Matching MODIS observations			15.0		13.5	12.0
	• Phase (assessed using the month of maximum LAI)	Low	Low		6.0	5.1	4.2
	• Maximum (derived separately for major biome classes)	Moderate	Low		5.0	4.6	4.3
NPP	• Mean (derived separately for major biome classes)	Moderate	Low		4.0	3.8	3.5
	Comparisons with field observations and satellite products			10.0		8.0	8.2
	• Matching EMDI Net Primary Production observations	High	High		2.0	1.5	1.6
	• EMDI comparison, normalized by precipitation	Moderate	Moderate		4.0	3.0	3.4
	• Correlation with MODIS ( $r^2$ )	High	Low		2.0	1.6	1.4
CO <sub>2</sub> annual cycle	• Latitudinal profile comparison with MODIS ( $r^2$ )	High	Low		2.0	1.9	1.8
	Matching phase and amplitude at Globalview flash sites			15.0		10.4	7.7
	• 60°–90°N	Low	Low		6.0	4.1	2.8
	• 30°–60°N	Low	Low		6.0	4.2	3.2
Energy & CO <sub>2</sub> fluxes	• 0°–30°N	Moderate	Low		3.0	2.1	1.7
	Matching eddy covariance monthly mean observations			30.0		17.2	16.6
	• Net ecosystem exchange	Low	High		6.0	2.5	2.1
	• Gross primary production	Moderate	Moderate		6.0	3.4	3.5
	• Latent heat	Low	Moderate		9.0	6.4	6.4
Transient dynamics	• Sensible heat	Low	Moderate		9.0	4.9	4.6
	Evaluating model processes that regulate carbon exchange on decadal to century timescales			30.0		16.8	13.8
	• Aboveground live biomass within the Amazon Basin	Moderate	Moderate		10.0	5.3	5.0
	• Sensitivity of NPP to elevated levels of CO <sub>2</sub> : comparison to temperate forest FACE sites	Low	Moderate		10.0	7.9	4.1
	• Interannual variability of global carbon fluxes: comparison with TRANSCOM	High	Low		5.0	3.6	3.0
	• Regional and global fire emissions: comparison to GFEDv2	High	Low		5.0	0.0	1.7

Total: 100.0      65.9      58.3

(Randerson et al., 2009)

# Biogeochemistry–Climate Feedbacks Scientific Focus Area



# ILAMB Prototype Diagnostics System

An initial ILAMB prototype has been developed by Mingquan Mu at UCI.

► Current variables:

Aboveground live biomass (North America FIA, tropical Saatchi et al.), Burned area (GFED3), CO<sub>2</sub> (NOAA GMD, Mauna Loa), Global net land flux (GCP), Gross primary production (Fluxnet-MTE), Leaf area index (AVHRR, MODIS), Net ecosystem exchange (Fluxnet), Respiration (Fluxnet), Soil C (HWSD, NCSCDv2), Evapotranspiration (LandFlux, GLEAM, MODIS), Latent heat (Fluxnet-MTE), Soil moisture (ESA), Terrestrial water storage change (GRACE), Precipitation (GPCP2), Albedo (MODIS, CERES), Surface up/down SW/LW radiation (CERES, WRMC.BSRN), Sensible heat (Fluxnet), Surface air temperature (CRU).

► Graphics and scoring systems:

- Annual mean, Bias, RMSE, seasonal cycle, spatial distribution, interannual coeff. of variation and variability, long-term trend scores
- Global maps, variable to variable, and time series comparisons

► Software:

Freely distributed, designed to be user friendly and to enable easy addition of new variables  
(Mu, Hoffman, Riley, Koven, Lawrence, Randerson)

# ILAMB Prototype Layout: Global Variables

## Global Variables ([Info](#))

	MeanModel	bcc-csm1-1-m	BNU-ESM	CanESM2	CESM1-BGC	GFDL-ESM2G	HadGEM2
<u>Aboveground Live Biomass</u>	0.88	-	0.14	0.81	0.68	0.81	0.86
<u>Burned Area</u>	0.41	-	-	-	0.37	-	-
<u>Carbon Dioxide</u>	0.88	-	0.53	0.94	0.86	0.96	-
<u>Global Net Land Flux</u>	0.25	-	0.25	0.32	0.32	0.49	0.63
<u>Gross Primary Production</u>	0.80	0.74	0.74	0.74	0.77	0.72	0.75
<u>Leaf Area Index</u>	0.59	0.64	0.30	0.78	0.53	0.33	0.53
<u>Net Ecosystem Exchange</u>	0.36	0.29	0.19	0.16	0.28	0.64	0.28
<u>Ecosystem Respiration</u>	0.78	0.71	0.78	0.75	0.74	0.70	0.77
<u>Soil Carbon</u>	0.71	-	0.35	0.73	0.31	0.74	0.63
<u>Summary</u>	0.63	0.59	0.41	0.65	0.54	0.67	0.64
<u>Evapotranspiration</u>	0.75	0.83	0.74	0.82	0.73	0.76	0.77
<u>Latent Heat</u>	0.77	0.79	0.71	0.80	0.71	0.72	0.71
<u>Soil Moisture</u>	0.18	0.17	0.20	0.21	0.19	0.18	0.21
<u>Terrestrial Water Storage Change</u>	0.25	0.29	0.25	0.26	0.25	0.24	0.25
<u>Precipitation</u>	0.82	0.83	0.82	0.82	0.86	0.86	0.90
<u>Summary</u>	0.55	0.58	0.54	0.58	0.55	0.55	0.57
<u>Albedo</u>	0.76	0.74	0.75	0.77	0.80	0.76	0.79

# ILAMB Prototype Layout: Variable to Variable

## Variable to Variable Relationships

	<b>Relationship</b>	<b>Benchmark</b>	<b>MeanModel</b>	<b>bcc-csm1-1-m</b>	<b>BNU-ESM</b>	<b>CanESM2</b>	<b>CESM1-BGC</b>	<b>GFDL-CM2.3</b>
<u>Precipitation vs. Burned Area</u>	function_bar	<u>1</u>	<u>0.57</u>	-	-	-	<u>0.57</u>	
<u>Precipitation vs. Gross Primary Production</u>	function_bar	<u>1</u>	<u>0.91</u>	<u>0.92</u>	<u>0.93</u>	<u>0.50</u>	<u>0.93</u>	<u>0.</u>
<u>Surface Air Temperature vs. Burned Area</u>	function_bar	<u>1</u>	<u>0.00</u>	-	-	-	<u>0.08</u>	
<u>Surface Air Temperature vs. Gross Primary Production</u>	function_bar	<u>1</u>	<u>0.62</u>	<u>0.50</u>	<u>0.45</u>	<u>0.92</u>	<u>0.50</u>	<u>0.</u>
<u>Surface Downward SW Radiation vs. Gross Primary Production</u>	function_bar	<u>1</u>	<u>0.85</u>	<u>0.74</u>	<u>0.91</u>	<u>0.64</u>	<u>0.81</u>	<u>0.</u>
<u>Surface Net SW Radiation vs. Gross Primary Production</u>	function_bar	<u>1</u>	<u>0.72</u>	<u>0.72</u>	<u>0.72</u>	<u>0.86</u>	<u>0.79</u>	<u>0.</u>
<u>Overall</u>			<u>0.61</u>	<u>0.72</u>	<u>0.75</u>	<u>0.73</u>	<u>0.61</u>	<u>0.</u>

# ILAMB Prototype Layout: Time Series

## Time Series Comparisons

	Benchmark
<b>Burned Area</b>	<b>GFED3</b> [Giglio et al. (2010)]
<b>Carbon Dioxide</b>	<b>NOAA.GMD</b> [Dlugokencky et al. (2013)]
<b>Gross Primary Production</b>	<b>FLUXNET</b> [Lasslop et al. (2010)]
<b>Net Ecosystem Exchange</b>	<b>FLUXNET</b> [Lasslop et al. (2010)]
<b>Ecosystem Respiration</b>	<b>FLUXNET</b> [Lasslop et al. (2010)]
<b>Surface Downward SW Radiation</b>	<b>WRMC.BSRN</b> [Konig-Langlo et al. (2013)]
<b>Surface Upward SW Radiation</b>	<b>WRMC.BSRN</b> [Konig-Langlo et al. (2013)]
<b>Surface Net SW Radiation</b>	<b>WRMC.BSRN</b> [Konig-Langlo et al. (2013)]
<b>Surface Downward LW Radiation</b>	<b>WRMC.BSRN</b> [Konig-Langlo et al. (2013)]
<b>Surface Upward LW Radiation</b>	<b>WRMC.BSRN</b> [Konig-Langlo et al. (2013)]
<b>Surface Net LW Radiation</b>	<b>WRMC.BSRN</b> [Konig-Langlo et al. (2013)]

# ILAMB Live Demo

# Community Model Benchmarking

## Community Involvement Is Key to Success!

- ▶ Our international collaboration has made significant progress on development of metrics in the ILAMB prototype.
- ▶ Our **BGC-Feedbacks Project** is developing new model–data analysis studies for terrestrial and now marine biogeochemistry (see <http://www.bgc-feedbacks.org/>).
- ▶ We have proposed an **ILAMB Town Hall** at the upcoming American Geophysical Union (AGU) Fall Meeting in December.
- ▶ We are planning another community-wide meeting on model metrics and diagnostics in Washington, DC, USA in spring 2016.

**International Land Model Benchmarking (ILAMB) Project**

<http://www.ilamb.org/>

**Contact:** Forrest M. Hoffman <[forrest@climatemodeling.org](mailto:forrest@climatemodeling.org)>

# Acknowledgments



U.S. DEPARTMENT OF  
**ENERGY**

---

Office of Science



This research was sponsored by the Climate and Environmental Sciences Division (CESD) of the Biological and Environmental Research (BER) Program in the U. S. Department of Energy Office of Science and the National Science Foundation (AGS-1048890). This research used resources of the Oak Ridge Leadership Computing Facility (OLCF) at Oak Ridge National Laboratory (ORNL), which is managed by UT-Battelle, LLC, for the U. S. Department of Energy under Contract No. DE-AC05-00OR22725.

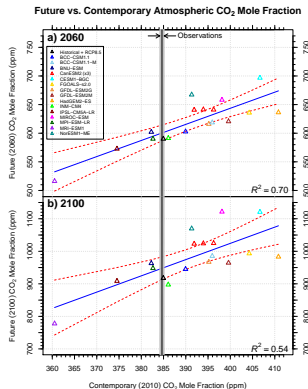
I wish to acknowledge the World Climate Research Programme's Working Group on Coupled Modelling, which is responsible for CMIP, and thank the climate modeling groups for producing and making available their model output. For CMIP the U. S. Department of Energy's Program for Climate Model Diagnosis and Intercomparison provides coordinating support and led development of software infrastructure in partnership with the Global Organization for Earth System Science Portals.

# References

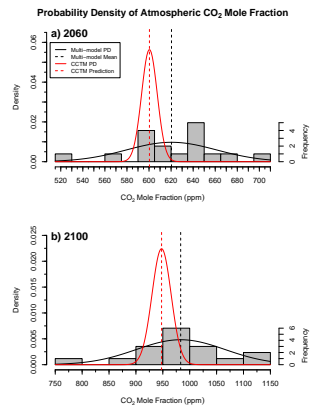
- R. J. Andres, J. S. Gregg, L. Losey, G. Marland, and T. A. Boden. Monthly global emissions of carbon dioxide from fossil fuel consumption. *Tellus B*, 63(3):309–327, July 2011. doi:10.1111/j.1600-0889.2011.00530.x.
- R. J. Andres, T. A. Boden, F.-M. Bréon, P. Ciais, S. Davis, D. Erickson, J. S. Gregg, A. Jacobson, G. Marland, J. Miller, T. Oda, J. G. J. Olivier, M. R. Raupach, P. Rayner, and K. Treanton. A synthesis of carbon dioxide emissions from fossil-fuel combustion. *Biogeosci.*, 9(5):1845–1871, May 2012. doi:10.5194/bg-9-1845-2012.
- P. M. Cox, D. Pearson, B. B. Booth, P. Friedlingstein, C. Huntingford, C. D. Jones, and C. M. Luke. Sensitivity of tropical carbon to climate change constrained by carbon dioxide variability. *Nature*, 494(7437):341–344, Feb. 2013. doi:10.1038/nature11882.
- A. Hall and X. Qu. Using the current seasonal cycle to constrain snow albedo feedback in future climate change. *Geophys. Res. Lett.*, 33(3):L03502, Feb. 2006. doi:10.1029/2005GL025127.
- F. M. Hoffman, J. T. Randerson, V. K. Arora, Q. Bao, P. Cadule, D. Ji, C. D. Jones, M. Kawamiya, S. Khatiwala, K. Lindsay, A. Obata, E. Shevliakova, K. D. Six, J. F. Tjiputra, E. M. Volodin, and T. Wu. Causes and implications of persistent atmospheric carbon dioxide biases in Earth System Models. *J. Geophys. Res. Biogeosci.*, 119(2):141–162, Feb. 2014. doi:10.1002/2013JG002381.
- S. Khatiwala, T. Tanhua, S. Mikaloff Fletcher, M. Gerber, S. C. Doney, H. D. Graven, N. Gruber, G. A. McKinley, A. Murata, A. F. Ríos, and C. L. Sabine. Global ocean storage of anthropogenic carbon. *Biogeosci.*, 10(4):2169–2191, Apr. 2013. doi:10.5194/bg-10-2169-2013.
- Y. Q. Luo, J. T. Randerson, G. Abramowitz, C. Bacour, E. Blyth, N. Carvalhais, P. Ciais, D. Dalmonech, J. B. Fisher, R. Fisher, P. Friedlingstein, K. Hibbard, F. Hoffman, D. Huntzinger, C. D. Jones, C. Koven, D. Lawrence, D. J. Li, M. Mahecha, S. L. Niu, R. Norby, S. L. Piao, X. Qi, P. Peylin, I. C. Prentice, W. Riley, M. Reichstein, C. Schwalm, Y. P. Wang, J. Y. Xia, S. Zaehle, and X. H. Zhou. A framework for benchmarking land models. *Biogeosci.*, 9(10):3857–3874, Oct. 2012. doi:10.5194/bg-9-3857-2012.
- M. Meinshausen, S. Smith, K. Calvin, J. Daniel, M. Kainuma, J.-F. Lamarque, K. Matsumoto, S. Montzka, S. Raper, K. Riahi, A. Thomson, G. Velders, and D. P. van Vuuren. The RCP greenhouse gas concentrations and their extensions from 1765 to 2300. *Clim. Change*, 109(1):213–241, Nov. 2011. doi:10.1007/s10584-011-0156-z.
- J. T. Randerson, F. M. Hoffman, P. E. Thornton, N. M. Mahowald, K. Lindsay, Y.-H. Lee, C. D. Neivison, S. C. Doney, G. Bonan, R. Stöckli, C. Covey, S. W. Running, and I. Y. Fung. Systematic assessment of terrestrial biogeochemistry in coupled climate-carbon models. *Global Change Biol.*, 15(9):2462–2484, Sept. 2009. doi:10.1111/j.1365-2486.2009.01912.x.
- C. L. Sabine, R. A. Feely, N. Gruber, R. M. Key, K. Lee, J. L. Bullister, R. Wanninkhof, C. S. Wong, D. W. R. Wallace, B. Tilbrook, F. J. Millero, T.-H. Peng, A. Kozyr, T. Ono, and A. F. Rios. The oceanic sink for anthropogenic CO<sub>2</sub>. *Science*, 305(5682):367–371, July 2004. doi:10.1126/science.1097403.

# Emergent Constraint Developed from CMIP5 ESMs

An emergent constraint based on carbon inventories was applied to future atmospheric CO<sub>2</sub> projections from CMIP5 ESMs.



- ▶ Much of the model-to-model variation in projected CO<sub>2</sub> during the 21<sup>st</sup> century is tied to biases that existed during observational era.
- ▶ Model differences in the representation of concentration–carbon feedbacks and other slowly changing carbon cycle processes appear to be the primary driver of this variability.
- ▶ Range of temperature increases at 2100 slightly reduced, from  $5.1 \pm 2.2^\circ\text{C}$  for the full ensemble, to  $5.0 \pm 1.9^\circ\text{C}$  after applying the emergent constraint.



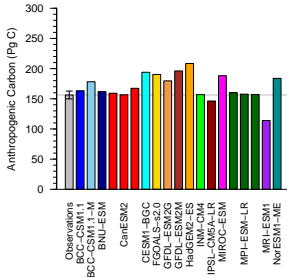
Best estimate using Mauna Loa CO<sub>2</sub>

- At 2060:  $600 \pm 14$  ppm, 21 ppm below the multi-model mean
- At 2100:  $947 \pm 35$  ppm, 32 ppm below the multi-model mean

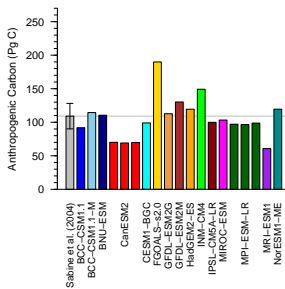
Hoffman, Forrest M., James T. Randerson, Vivek K. Arora, Qing Bao, Patricia Cadule, Duoying Ji, Chris D. Jones, Michio Kawamiya, Samar Khatiwala, Keith Lindsay, Atsushi Obata, Elena Shevliakova, Katharina D. Six, Jerry F. Tjiputra, Evgeny M. Volodin, and Tongwen Wu. February 2014. "Causes and Implications of Persistent Atmospheric Carbon Dioxide Biases in Earth System Models." *J. Geophys. Res. Biogeosci.*, 119(2):141–162. doi:10.1002/2013JG002381. *Most downloaded JGR-B paper for February 2014.*

# Model inventory comparison with Sabine et al. (2004)

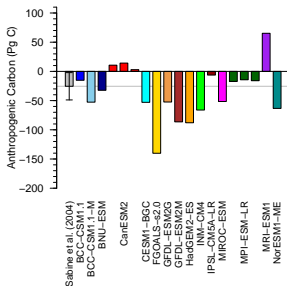
Atmosphere (1850–1994)



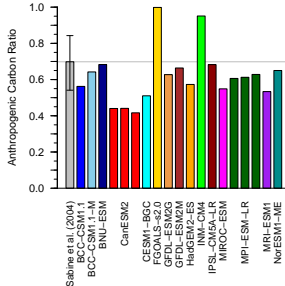
Ocean (1850–1994)



Land (1850–1994)



Ocean/Atmosphere (1850–1994)



# Implications for CO<sub>2</sub>, Radiative Forcing, and Temperature

Model	CO <sub>2</sub> Mole Fraction (ppm)			Radiative Forcing (W m <sup>-2</sup> )			Cumulative ΔT (°C)			ΔT Bias (°C)		
	2010	2060	2100	2010	2060	2100	2010	2060	2100	2010	2060	2100
BCC-CSM1.1	390	603	945	1.70	4.03	6.43	0.97	2.39	4.02	0.03	0.02	-0.01
BCC-CSM1.1-M	396	619	985	1.78	4.16	6.65	1.04	2.49	4.16	0.10	0.12	0.13
BNU-ESM	382	602	963	1.59	4.02	6.53	0.90	2.33	4.07	-0.04	-0.04	0.04
CanESM2 r1	394	641	1024	1.75	4.36	6.86	0.98	2.58	4.30	0.04	0.21	0.27
CanESM2 r2	392	641	1023	1.72	4.35	6.85	0.98	2.57	4.30	0.04	0.20	0.27
CanESM2 r3	396	641	1025	1.78	4.35	6.87	1.01	2.58	4.30	0.07	0.21	0.27
CESM1-BGC	407	697	1121	1.92	4.80	7.34	1.12	2.85	4.64	0.18	0.48	0.61
FGOALS-s2.0	404	636	993	1.89	4.31	6.70	1.09	2.57	4.23	0.15	0.20	0.20
GFDL-ESM2G	395	616	967	1.77	4.14	6.56	1.04	2.49	4.12	0.10	0.12	0.09
GFDL-ESM2M	400	621	964	1.83	4.18	6.54	1.09	2.52	4.13	0.15	0.15	0.10
HadGEM2-ES	411	636	983	1.98	4.31	6.64	1.18	2.60	4.20	0.24	0.23	0.17
INM-CM4	386	591	897	1.64	3.92	6.15	0.92	2.36	3.86	-0.02	-0.01	-0.17
IPSL-CM5A-LR	375	573	908	1.48	3.75	6.22	0.86	2.21	3.87	-0.08	-0.16	-0.16
MIROC-ESM	398	658	1121	1.81	4.50	7.35	1.06	2.67	4.58	0.12	0.30	0.55
MPI-ESM-LR r1	383	590	948	1.60	3.91	6.45	0.95	2.31	4.03	0.01	-0.06	0.00
MRI-ESM1	361	516	778	1.28	3.20	5.39	0.74	1.89	3.33	-0.20	-0.48	-0.70
NorESM1-ME	391	667	1070	1.72	4.57	7.09	0.98	2.68	4.46	0.04	0.31	0.43
Multi-model Mean	392	621	980	1.72	4.18	6.63	1.00	2.48	4.17	0.06	0.11	0.14
CCTM Estimate	385	600	948	1.62	4.01	6.45	0.94	2.37	4.03	—	—	—
Historical + RCP 8.5	385	590	917	1.63	3.91	6.27	0.94	2.32	3.93	0.00	-0.05	-0.10